LUND UNIVERSITY

Measuring techniques in induced polarisation imaging

Dahlin, Torleif; Leroux, Virginie; Nissen, J

Link to publication

Total number of authors:
3

Measuring techniques in induced polarisation imaging

Torleif Dahlin [a],*, Virginie Leroux [a], Johan Nissen [b,1]

[a]*Department of Geotechnology, Institute of Technology, Lund University, Box 118, S-221 00 Lund, Sweden*
[b]*Malå Geoscience Raycon AB, Sturev. 3, 17756 Järfälla, Sweden*

Abstract

Multi-electrode geoelectrical imaging has become very popular and is used for many different purposes. For some of these, the inclusion of IP data would be desirable as it would allow the interpreter to distinguish between, e.g. sand formations with saltwater infiltration and clay formations or help delineate landfills. However, present-day IP measuring techniques require the use of nonpolarisable potential electrodes and special wire layout and are thus cumbersome and expensive. In this paper, we suggest making IP measurements with multi-electrode cables and just one set of steel electrodes. The polarisation potentials on the potential electrodes are corrected for by subtracting the polarisation potential measured when no primary current and no IP signal are present. Test measurements indicate that the polarisation potentials vary slowly and that the correction procedure is feasible. At two sites in southern Sweden, we have compared measurements with only stainless steel electrodes and measurements with both stainless steel and Pb–PbCl nonpolarisable electrodes using one or two sets of multicore cables, respectively. Almost no difference between the two data sets was observed. At one site, the charge-up effect on the potential electrodes was not important, while at the other site, the correction procedure was crucial. Though only two sites have been studied so far, it seems that time-domain IP imaging measurements can be taken with only steel electrodes and ordinary multicore cables. Coupling in the multicore cables has not presented any problems at the investigated sites where grounding resistances were moderate, making the coupling effect small. High grounding resistance sites have not yet been investigated.
© 2002 Published by Elsevier Science B.V.

1. Introduction

Resistivity imaging has become increasingly popular for engineering and environmental applications since it is a cost-efficient means for, e.g. water or environmental exploration down to moderate depths (e.g. Overmeeren and Ritsema, 1988; Griffiths et al., 1990; Dahlin, 1993, 1996). However, ambiguity in the geological interpretation is a limiting factor. For example, in a sandy sedimentary formation, a low resistivity anomaly can be caused either by an increase in ion content in the water formation, a higher water content or a higher clay content. Such cases could possibly be distinguished if we also knew the chargeability of the formation. Initially designed for mining purposes, the induced polarisation method has also long been used in groundwater and environmental applications (Vacquier et al., 1957; Vanhala, 1999; Carlson et al., 1999)

---

* Corresponding author.
E-mail addresses: torleif.dahlin@tg.lth.se (T. Dahlin),
virginie@tg.lth.se (V. Leroux), jni@malags.se (J. Nissen).
[1] Formerly at ABEM Instrument AB.

and has recently regained interest (e.g. Weller et al., 1996; Slater and Lesmes, 2002).

Induced polarisation measurements can be performed either in the frequency or time domain. In the time domain, one measures the decay of the voltage between the two potential electrodes after the current has been turned off. It is characterised by the apparent chargeability M, which can be expressed, for example, in mV/V as:

$$M = \frac{1}{V_0[t_{i+1} - t_i]} \int_{t_i}^{t_{i+1}} V(t)\mathrm{d}t$$

The potential $V(t)$ is integrated in the time window $[t_i, t_{i+1}]$, then divided by the duration of the window and by the DC potential V_0, used to calculate the apparent resistivity.

The apparent chargeability can be computed from the resistivity calculation considering that the potential observed in a polarisable medium can be calculated as the potential that would be observed in a nonpolarisable medium of conductivity $\sigma_i' = \sigma_i(1 - m_i)$ where σ_i and m_i are the conductivity and the chargeability of the polarisable medium. In that, we follow the formulation given by Seigel (1959).

Inverse modelling based on the above approach has been implemented in commercially available software like Res2dinv (Loke and Barker, 1996; Loke, 1999), where the chargeabilities are interpreted relatively to the resistivities, the computation of the resistivities remaining independent.

Because of their potential to resolve ambiguities, and the interpretation software being available, it would be preferable to have as many chargeability as resistivity data points, thus extending the concept of "geoelectric imaging".

Ideally, one would use only one set of equipment (electrodes, cables and instrument) for both types of measurements. Until now, IP measurements have been costly and quite heavy to carry out. Since they can more easily be disturbed, several precautions have to be taken to obtain good quality data.

The main difficulty is that we deal with potentially intricate phenomena from which we want to extract the apparent chargeability. First, the signal is often weak, in any case, much lower than the direct current potential, which is itself sometimes small compared to the charge-up effect potential measured on electro-

des that have previously been used to inject current (Dahlin, 2000). All these reasons make it necessary to use a voltmeter with high resolution and a powerful transmitter.

The capacitive and the inductive coupling in the cables have to be considered. The capacitive coupling is likely to be relatively stable and decreases quickly with increasing distances between transmitting cables and potential reading cables, and increasing the cable separation will reduce it. One must also consider the inductive coupling between the cables via the ground, which is indeed the signal studied in transient EM methods. It is often assumed that its influence is felt predominantly at earlier times and that it quickly decreases, so that it could be safe to consider the decay curve only after a certain delay (e.g. Bertin and Loeb, 1976; Sumner, 1976). Its relative importance can be estimated via the calculation of the induction number depending on the frequency, the conductivity of the ground and the length of the cables. It can also be estimated in simple geological situations and if it is not too high, these calculations can to a certain extent be used to correct for it, even if it can, in some cases, remain extremely difficult to completely separate IP from inductive transients (see, e.g. Wait and Gruska, 1986). This led to the preferential use of the dipole–dipole configuration and to avoid the use of multicore cables for IP measurements. However, these may still be possible to use: if the grounding resistances are low, then the capacitive coupling between two conductors, even close to each other, could be low enough to allow good quality data.

Part of the measured signal is also due to the charge on the potential electrodes, which can have two origins. It can be because the potential electrodes have previously been used to transmit current. In that case, a strong potential, much higher than the direct current potential itself, can appear at the electrodes. In places it can take several tens of minutes for the charge-up to die out. In resistivity surveying these effects can be efficiently suppressed by the use of a plus-minus-plus type of measurement cycle, if potential measurement immediately after transmitting current through the electrodes is avoided via suitable protocols (Dahlin, 2000). A charge also appears at the contact between the soil and the electrode, depending on electrochemical phenomena (see, for instance, Vanhala and Soininen (1995) for some examples of natural
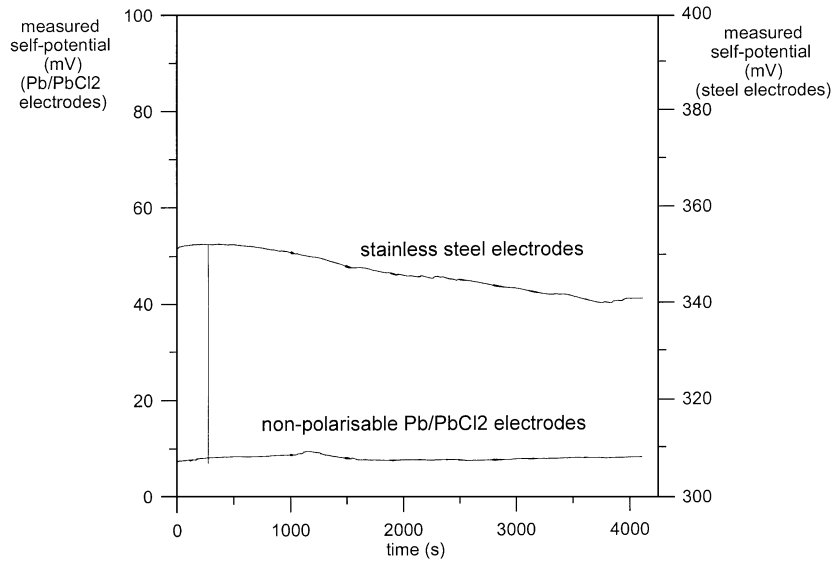
Fig. 1. Example of noise registration of potentials between two pairs of lead chloride electrodes and two pairs of stainless steel electrodes. The registration was carried on a lawn within the Lund University campus.

potentials observed with different electrode types). This is the reason why nonpolarisable electrodes are usually used, since the potential difference due to the charge-up is much smaller and relatively stable.

In spite of these obstacles, it appears possible to use stainless steel electrodes and multicore cables like for DC resistivity measurements, at least in favourable conditions, but taking some particular precautions.

Fig. 2. Detail from noise registration in Fig. 1.

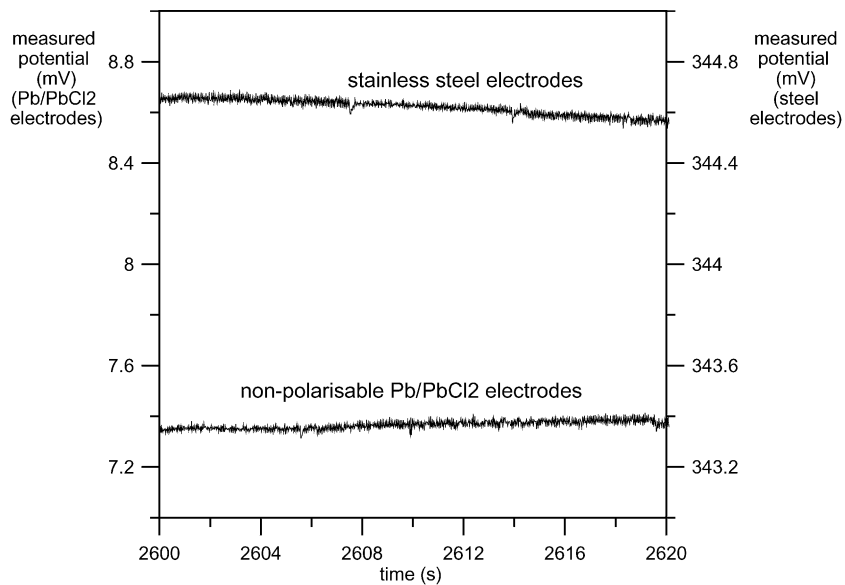If we can assume that the noise at the electrodes is a smoothly varying function with time, and we can have a reasonable, even partial estimation of it, then it should be possible to correct.

2. Electrode types and noise characteristics

2.1. Noise measurements

We had at our disposal two different kinds of electrodes: standard stainless steel electrodes and non-polarisable lead–lead chloride electrodes. The first ones were pegs of 0.5 m length, and the second ones were composed of a lead wire placed in a small plastic tube filled with a gypsum plaster prepared with water saturated with $PbCl_2$ and NaCl. Seventy pieces were made especially for this study, after a recipe given by Petiau and Dupis (1980). The length of the cylindrical

tube is 60 mm and the diameter is 20 mm. It should be noted that their construction makes these electrodes relatively robust, handy, easy-to-use, and that they can be placed either horizontally or vertically into the ground.

To estimate the noise we could expect from the electrodes, we made a little experiment on a small lawn at the Lund University Campus, a place that is not especially protected from anthropogenic noise, since there are many buried cables and electrical installations in the vicinity. Two steel electrodes and two lead–lead chloride electrodes were placed into the ground, with a spacing of 50 cm. The natural potentials were recorded for several hours, using two Lawson Labs AD201 24 bit A/D converters, one for each pair of electrodes with an internal data rate set to 50 Hz, and the measurements started right after the electrodes had been put in place.

The experiment was repeated several times at different locations. Fig. 1 presents one example. The
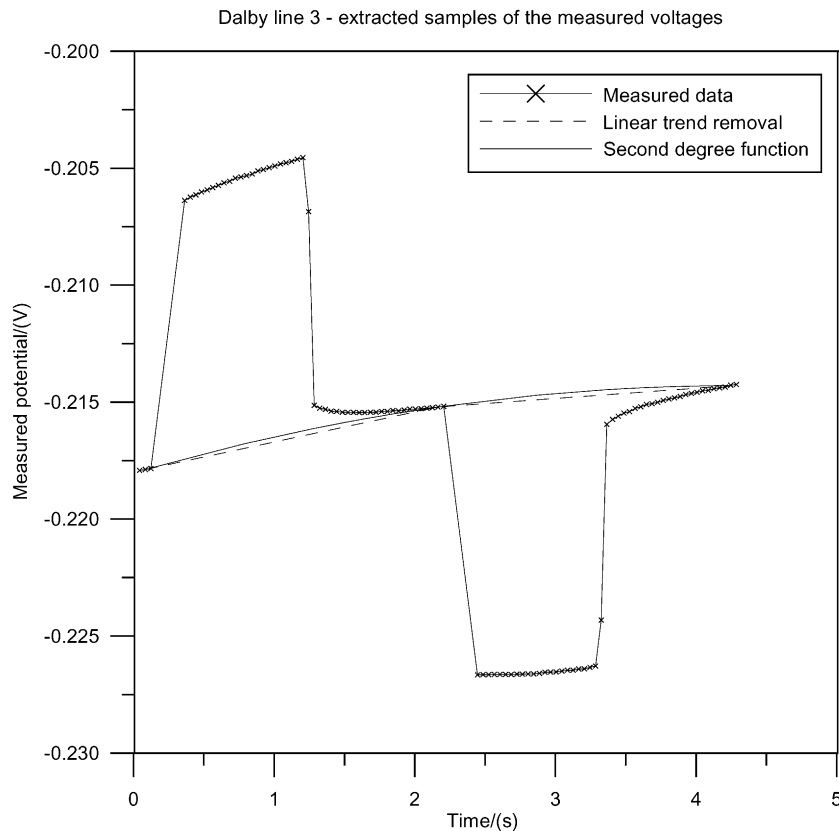

Fig. 3. Principle of the low-frequency trend correction: one example for the potential measured over an injection cycle on a steel electrode.

graph is constructed using two scales shifted relatively to each other because the steel electrodes present a much stronger zero offset (around 350 mV), whereas it is only about 8 mV for the nonpolarisable ones. The large-scale temporal drift is more visible for the steel electrodes, which also show an isolated spike whose origin is not clear. Looking at a detail lasting only 20 s like the one shown in Fig. 2, we can see that the high-frequency noise measured with the two types of electrodes is in the same range and very similar in character. This behaviour has also been noted by authors like Vanhala and Soininen (1995) for various kinds of electrodes.

It seems that this high-frequency noise of apparently stochastic occurrence cannot be avoided, whatever electrodes are used, but it should be possible to correct for a significant part of the low-frequency drift.

In order to correct the chargeability data for electrode drift, it is necessary to measure the background potential immediately before current is transmitted. Assuming that the signal-off time has been long enough to reach the point where the induced polarisation effect has almost disappeared, we can use the last points of the time periods without injection to estimate the potential on the electrodes. Then, inter-polating between these points can provide a way of correcting from it, before integrating the potential to calculate the chargeability windows. The principle of this correction is illustrated in Fig. 3, which shows an example of the potential measured over an injection cycle on a pair of stainless steel electrodes.

2.2. Assessment of the efficiency of the correction

We performed a test at the Lund University Campus with the same equipment used at the Dalby test site and described below. The experimental set-up is described in Fig. 7. We had 21 stainless steel electro-
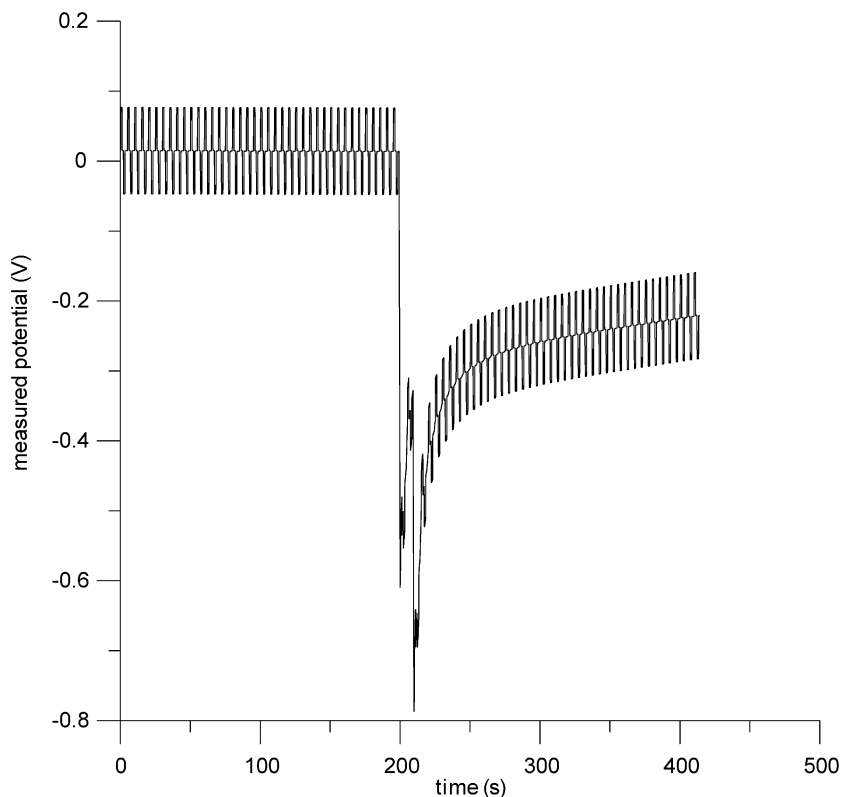

Fig. 4. Potential difference measured between two steel electrodes over 40 measurement cycles, before and after the perturbation by a reciprocal measurement (measured on a lawn at the Lund University Campus).

des and 21 lead–lead chloride electrodes, each set being connected to separate multicore cables. We selected 20 different measurement points in the Wenner configuration with a-spacings ranging from 6 to 12 m. Each point has been measured a number of times, before one reciprocal measurement was taken to charge the electrodes, after which the points were measured in the initial configuration again for a number of times (20 times with the steel electrodes, 5 times with the lead–lead chloride ones). Fig. 4 shows what happened to the potential measured with the steel electrodes.

The chargeability values were calculated in all cases for the time window of 80–180 ms after the current turn-off. A very good agreement between the values obtained either with the steel or lead–lead chloride electrodes can be observed before the disturbance and a few cycles after it. One example is given in Fig. 5. It can be noted that there are some data points with high noise levels for the lead–lead chloride electrodes that are not present in the steel electrode data, probably due to bad connection between the electrode and the multicore cable. The test shows that the correction for the charge-up effect, even if it is simple and based only on three points,

enabled us to retrieve a correct chargeability value from a potential strongly disturbed by the charge-up effect.

We also repeated the measurements with three different current levels, namely, 20, 100 and 200 mA, and we could see that the chargeability value did not vary, as illustrated in Fig. 6. Since we could obtain the same results using one or two separate multicore cables, the capacitive coupling has not been important.

It should be noted that this case is rather extreme, since it is usually possible to wait a few minutes before turning current electrodes into potential electrodes.

2.3. IP imaging experimental set-up

Two field tests were carried out in southern Sweden using two different versions of the ABEM Lund Imaging System. Like described in Fig. 7, in both cases, two relay switching units ES464 and two sets of electrode cables were used. Ordinary steel electrodes were connected to the first switching unit via one set of electrode cables, while lead–lead chloride electrodes were connected to the other switching unit via separate
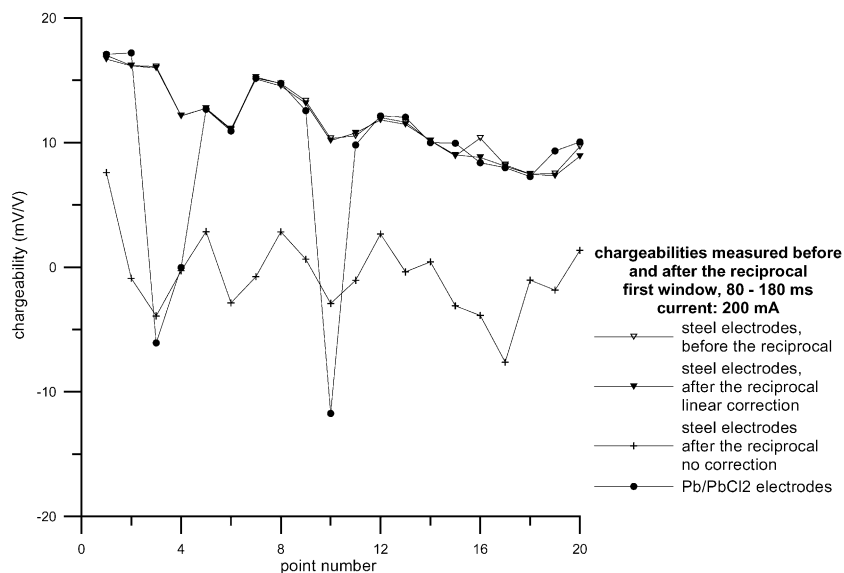

Fig. 5. Chargeabilities measured on a lawn at the Lund University Campus with steel electrodes, before and after charging them with a reciprocal measurement, compared to the ones measured with nonpolarisable electrodes.
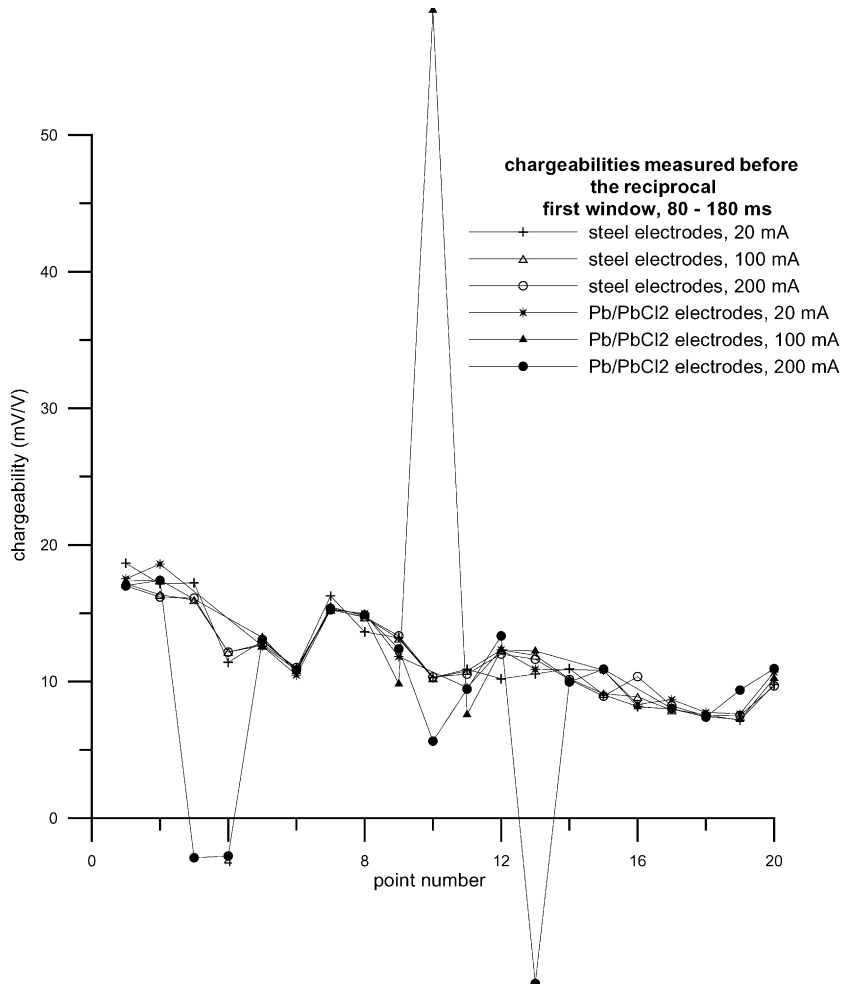
Fig. 6. Chargeabilities measured on a lawn at the Lund University Campus with two electrode types and three injection levels (the equipment used was the same as in Dalby).

electrode cables. Two sets of three standard electrode cables with 21 take-outs each were used, to give a total layout of 2×61 electrodes with overlapping take-outs at the cable ends. The two sets of electrode cables were laid out in parallel and separated by approximately 1 m. The current was injected into the ground through the steel electrodes, whereas both the steel electrodes (the same also used alternately for transmitting current) and the lead–lead chloride electrodes were used for simultaneous potential measurements.

At the Östra Odarslöv site, an ABEM Terrameter SAS 4000 was used for the measurements. It is a four-channel instrument with the transmitter integrated as

well as a computer, which can also control the switching units. At the Dalby Östra Mölla site, we used a research system built at Lund University, which consists of a Lawson Labs AD201 to measure the potentials (single channel), and of an ABEM Booster SAS2000 to transmit the current. A PC-compatible field computer also controlling the switching units controls the system.

2.4. Measurement protocols

Special measurement protocols were designed that allowed simultaneous measurements on matching pairs
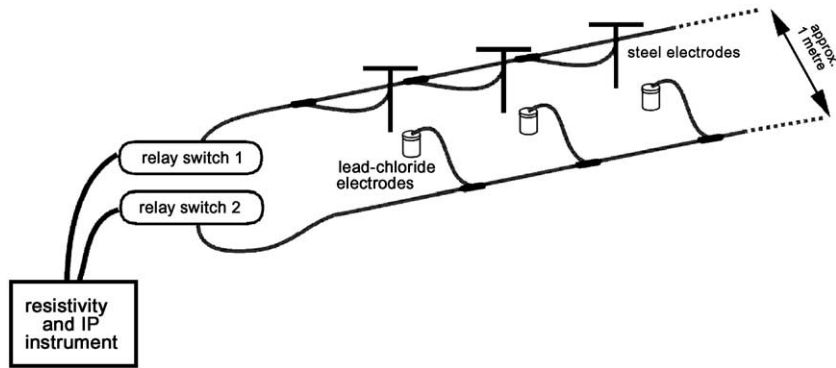
Fig. 7. Sketch of field layout used for tests with multi-electrode IP measurements. The arrangement allows simultaneous potential measurements on the steel electrodes and lead chloride electrodes, while current is being transmitted via the steel electrodes, provided a receiver equipped with at least two channels is used.

of steel and lead–lead chloride electrodes. The measuring sequence was also designed in order to minimise the disturbance caused by the "charge-up effect" on a current electrode (Dahlin, 2000). The time interval between the moment a steel electrode was used to transmit current and the moment it was used for measuring the potential was kept as long as possible.

In all cases, we used transmitting and measuring periods of 1 s each. The current intensity was 100 mA at Dalby, while it was 200 mA at Östra Odarslöv.

2.5. Array types

The Wenner array was used for the measurements presented here, and both normal and reciprocal data were recorded in order to allow estimations of the data quality in an objective way.

3. Dalby Östra Mölla test site

3.1. Site description

The test line was measured across a capped landfill situated within the village Dalby, known to stand out as a low resistive feature from previous research (Bernstone and Dahlin, 1997). The landfill consists of a former quarry filled up with waste, mainly from a local industry, and it was closed in the late 1960s. It is now a flat open green area lined by village residences.

The test site is situated on the Romeleåsen horst, one of the several uplifted blocks of the upper crust that are found in the southernmost part of Sweden. The horst is composed of Precambrian rocks, mainly gneiss. The clayey soil that covers the rock is thin and sometimes the gneiss outcrops at the surface. The degree of weathering is generally very low because Pleistocene glaciations have eroded the weathered rocks of former geological periods. Water-bearing fractures in the rock constitute an aquifer of importance. Fig. 8 shows a principal cross section of the area.

3.2. Results

The measurements were carried out using Wenner electrode spacings ranging between 4 and 48 m. The lead–lead chloride data were measured another day than the steel electrode data since only one channel
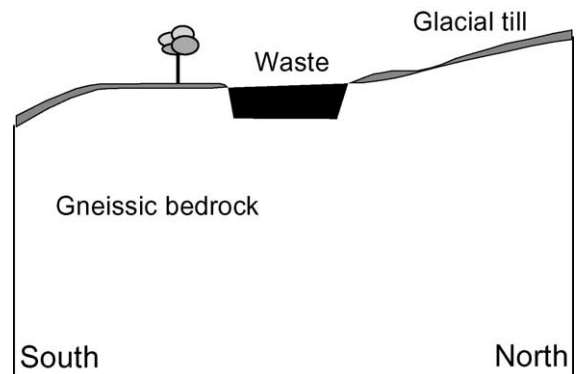
Fig. 8. A sketch principal cross section of the Dalby Östra Mölla landfill site (Bernstone and Dahlin, 1997).
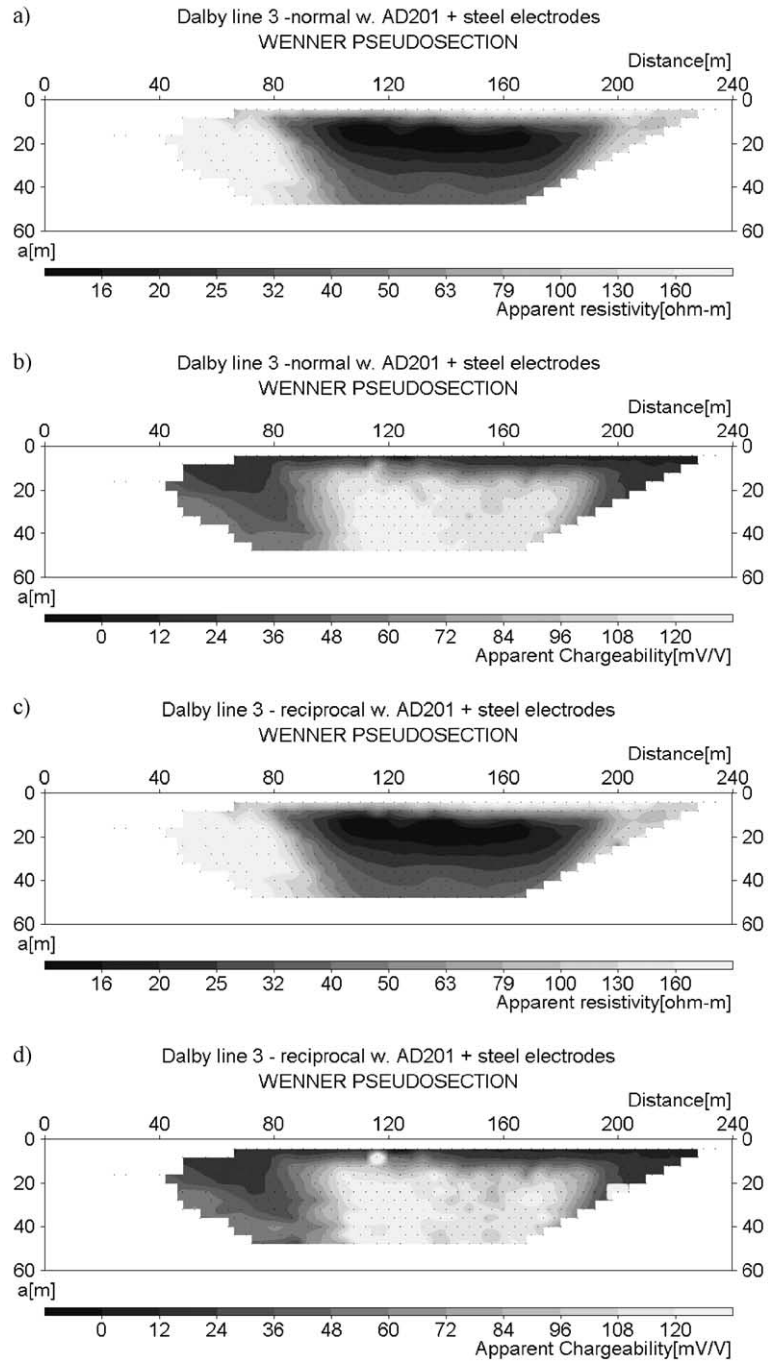
Fig. 9. Pseudosections measured with steel electrodes at Dalby Östra Mölla. Time window approximately 80–180 ms after current turn-off used for the chargeability (see discussion on low-pass filter effect). (a) Apparent resistivity measured with normal Wenner array. (b) Apparent chargeability measured with normal Wenner array. (c) Apparent resistivity measured with reciprocal Wenner array. (d) Apparent chargeability measured with reciprocal Wenner array.

was available in the experimental data acquisition system and for logistical reasons.

The results measured with steel electrodes are presented as pseudosections of apparent resistivity and apparent chargeability in Fig. 9a–d, where the upper two sections show data measured using normal Wenner array, and the lower show the corresponding ones for the reciprocal array. The time window, approximately 80–180 ms after current turn-off, was used for calculating the chargeability. Chargeabilities were also calculated for other time windows up to 1 s after current turn-off, and the results were similar but with smaller anomaly amplitude. The buried waste stands out as an anomalous feature with low resistivity and high chargeability. The apparent resistivity pseudosections (Fig. 9a and c) are very similar, with a mean/median difference of 0.4/0.2%. The apparent chargeability pseudosections (Fig. 9b and d) also

agree well, but with a somewhat noisier appearance for the reciprocal data set.

The agreement between the chargeabilities measured with the stainless steel and the lead chloride electrodes has been represented in Fig. 10 for the normal Wenner array, and in Fig. 11 for the reciprocal Wenner array. Apart from a few outliers, this agreement is quite good in both cases.

An analysis of the differences between the four corresponding apparent chargeability data sets is presented in Tables 1 and 2. In the analysis of the measurement errors, both the absolute errors and the relative errors are presented as they yield useful information in the cases presented here. However, in general, the relative errors for chargeability must be viewed with great caution, since for data measured over ground with no chargeability, the relative errors can become infinitely large even if the noise level is
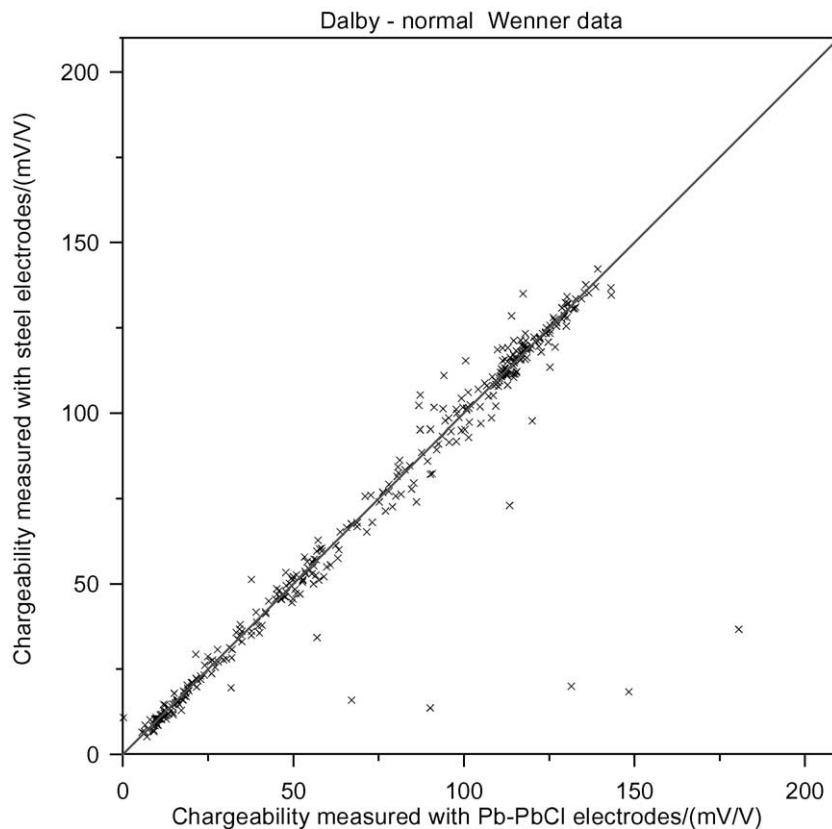

Fig. 10. Agreement between the normal Wenner chargeability values measured at Dalby with stainless steel and lead chloride electrodes.
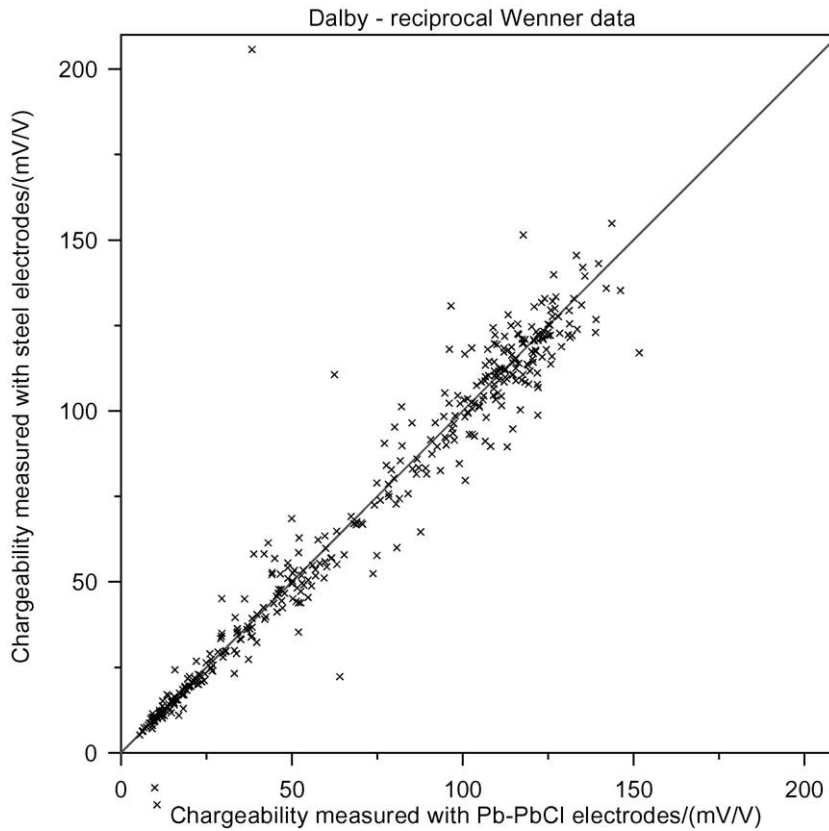
Fig. 11. Agreement between the reciprocal Wenner chargeability values measured at Dalby with stainless steel and lead chloride electrodes.

low. Thus, in most cases, an absolute error analysis approach would be preferable.

The mean/median differences between normal and reciprocal measurements are 3.7/1.6 mV/V for the steel electrodes, and 4.0/1.9 mV/V for the lead–lead chloride electrodes, respectively. This corresponds to a median relative difference of 3.2% between normal

Table 1
Statistics on the errors in apparent chargeability from the Dalby Östra Mölla test line

Type of error	Steel electrodes		Pb/PbCl$_2$ electrodes	
	Absolute (mV/V)	Relative (%)	Absolute (mV/V)	Relative (%)
Number of data	393	393	344	344
Minimum	0.0	0.0	0.0	0.0
Maximum	37.4	91.2	112.9	150.3
Mean	3.7	5.3	4	6.3
Median	1.6	3.2	1.9	3.4
Standard deviation	5	7.2	8.6	12.7

Error estimates from difference between normal and reciprocal measurements for steel electrodes and lead chloride electrodes, respectively. Time window is 100–180 ms after current turn-off.

Table 2
Statistics on the errors in apparent chargeability from the Dalby Östra Mölla test line

Type of error	Normal Wenner		Reciprocal Wenner	
	Absolute (mV/V)	Relative (%)	Absolute (mV/V)	Relative (%)
Number of data	350	350	384	384
Minimum	0.0	0.0	0.0	0.0
Maximum	111.5	147.4	167.4	137.2
Mean	3.2	6	5.6	8.4
Median	1.6	3	3	5.3
Standard deviation	8.1	13.7	10.4	11.4

Error estimates from difference between measurements using steel and lead chloride potential electrodes for normal and reciprocal Wenner, respectively. Time window is 100–180 ms after current turn-off.

and reciprocal measurements for the steel electrodes, and of 3.4% for the lead chloride. The measured levels are low, but the relative error values are quite similar for both types of electrodes. The comparison between the electrode types gives a difference of 3.2/1.6 mV/V for the normal array and 5.6/3.0 mV/V for the reciprocal array. This corresponds to a median difference between steel and lead–lead chloride electrodes of 3.0% for the normal array, and of 5.3% for the reciprocal one. In this case, the comparison shows that the difference is slightly smaller between the electrode types for the normal Wenner than between normal and reciprocal arrays for each type of electrode. The difference between the two reciprocal data sets is larger, and this may be attributed to the larger distance between the potential electrodes, raising the sensitivity to noise.

3.3. Charge-up effects and low-pass filtering

The electrode charge-up effects are very significant at the Dalby site. An example plot of the potentials measured on steel electrodes from four separate data points is shown in Fig. 12. Only two of the measurement points are shown complete, and the samples belonging to each data point are easily identified due to the difference in electrode charge-up effect. Two stacks were made on each of the data points shown here.

Fig. 13 shows a plot of the individual data samples recorded for a data point without significant IP-effect or electrode charge-up, to point out that the two first samples after the current turn-off are affected by the low-pass filter in the receiver, and thus discarded in the calculation of the apparent chargeability. The first sample used to calculate the chargeability is taken
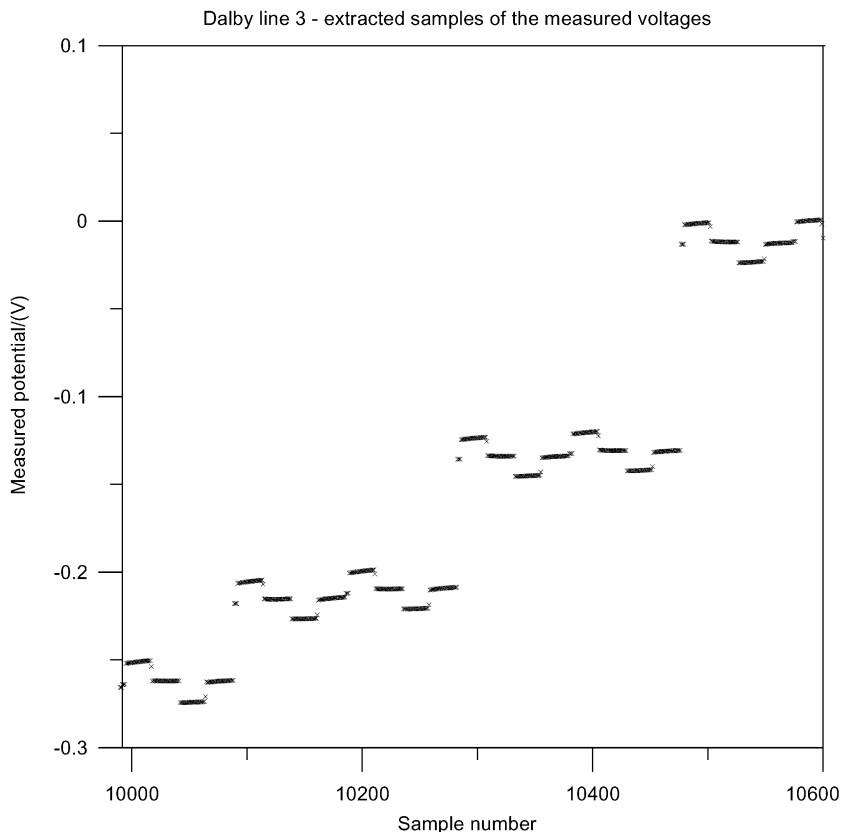

Fig. 12. Example plot of potentials measured on steel electrodes from four separate data points from the Dalby test line. Only two of the measurement points are shown complete, and the samples belonging to each data point are easily identified due to the difference in electrode charge-up effect. Two stacks were made on each of the data points shown here.

Dalby line 3 - extracted samples of the measured voltages
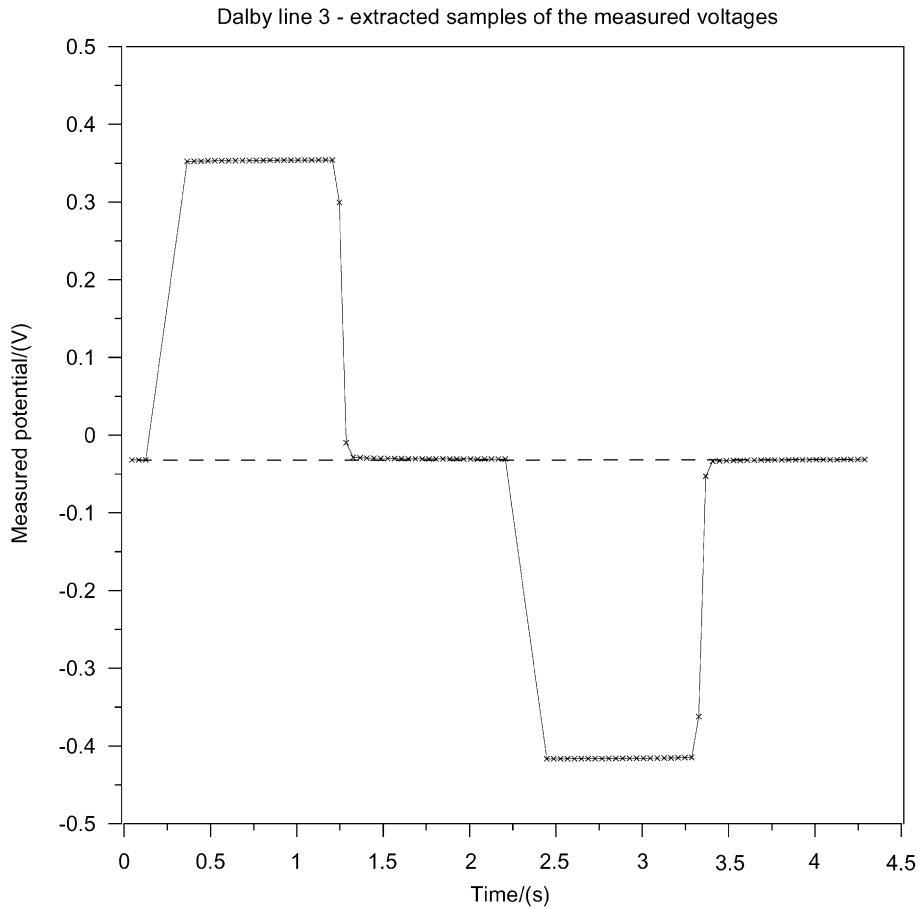
Fig. 13. Example plot of individual data samples recorded for a data point with small IP-effect and small electrode charge-up. Observe that the first two samples after current turn-off are affected by the low-pass filter in the receiver, and thus discarded in the calculation of the apparent chargeability.

Dalby line 3 - normal w. AD201 + steel electrodes w.o. drift correction
WENNER PSEUDOSECTION

Fig. 14. Apparent chargeability pseudosection measured with steel electrodes normal Wenner array at Dalby Östra Mölla, presented without electrode charge-up correction.

a)
Dalby line 3 - AD 201 + steel electrodes
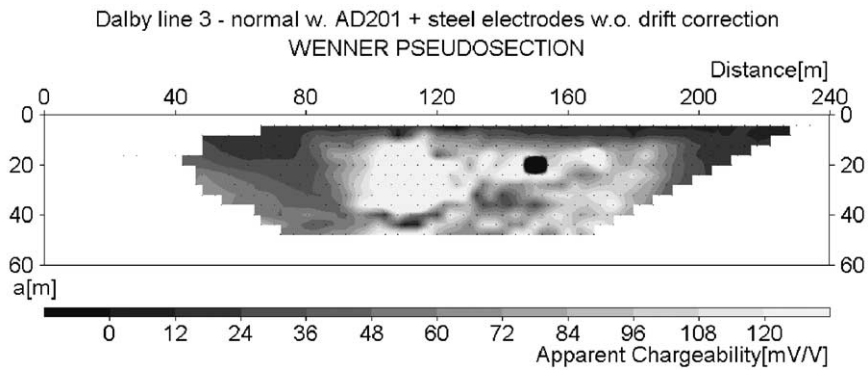NORMAL WENNER 2D INVERTED MODEL (mean residual 2.4%)

b)
Dalby line 3 - AD 201 + steel electrodes
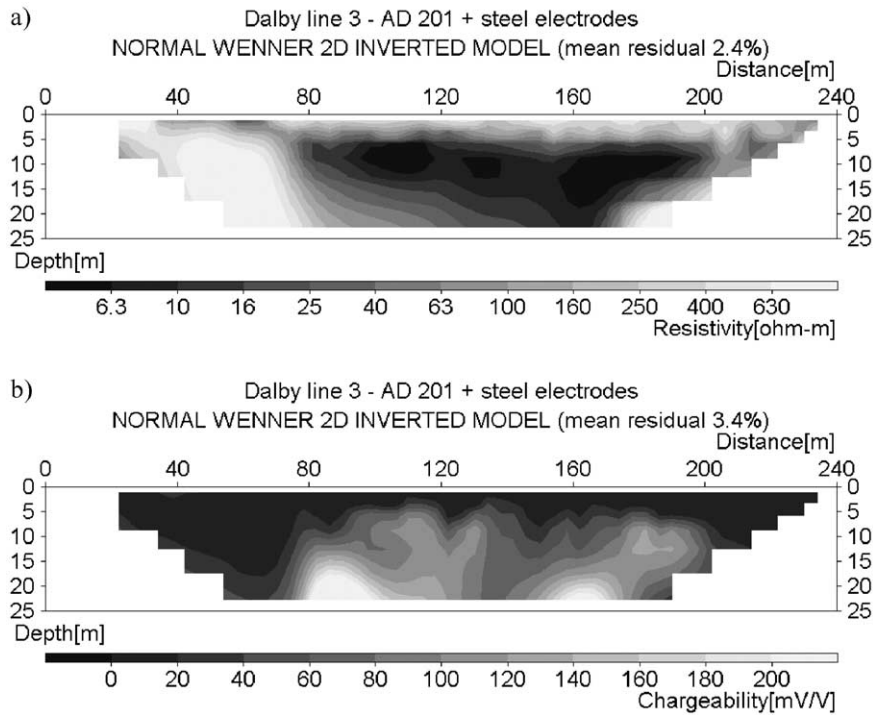NORMAL WENNER 2D INVERTED MODEL (mean residual 3.4%)

Fig. 15. Inverted sections based on data measured with normal Wenner array and steel electrodes at Dalby Östra Mölla. (a) Resistivity. (b) Chargeability.

around 80–100 m after current turn-off (a more exact definition of the delay time cannot be given due to the way the experimental system was built). However, as a result of the low-pass filtering of the A/D converter, much of the information recorded in the first data sample is characterised by times earlier than the actual time of the sample. Thus, the data recorded with the low-pass filter is the equivalent of measuring with a significantly shorter time if no low-pass filter was used. It is beyond the scope of this paper to go into details of

the exact mechanisms of this, but one evident benefit of using a relatively strong low-pass filtering is robustness against the noise picked along the cables. Similar effects in transient electromagnetic data acquisition systems, and a method to include the effect in inversion of the data has been discussed by Effersø et al. (1999).

Small electrode charge-up was an exception at the Dalby site, and an example of a data point with high chargeability as well as charge-up effects from this site was shown earlier in this paper (Fig. 3). The data
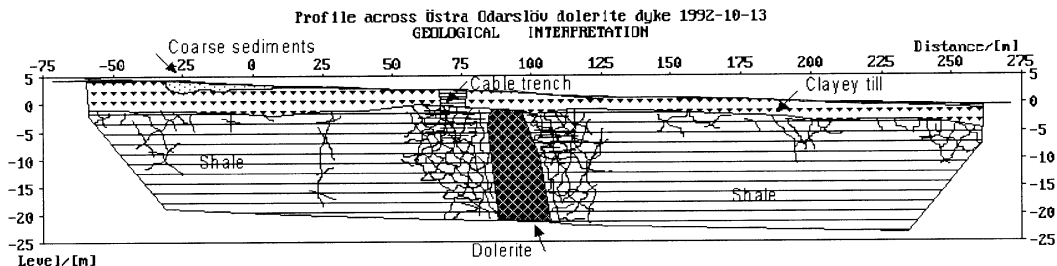
Fig. 16. A principal cross section of the Östra Odarslöv site (Dahlin, 1996).
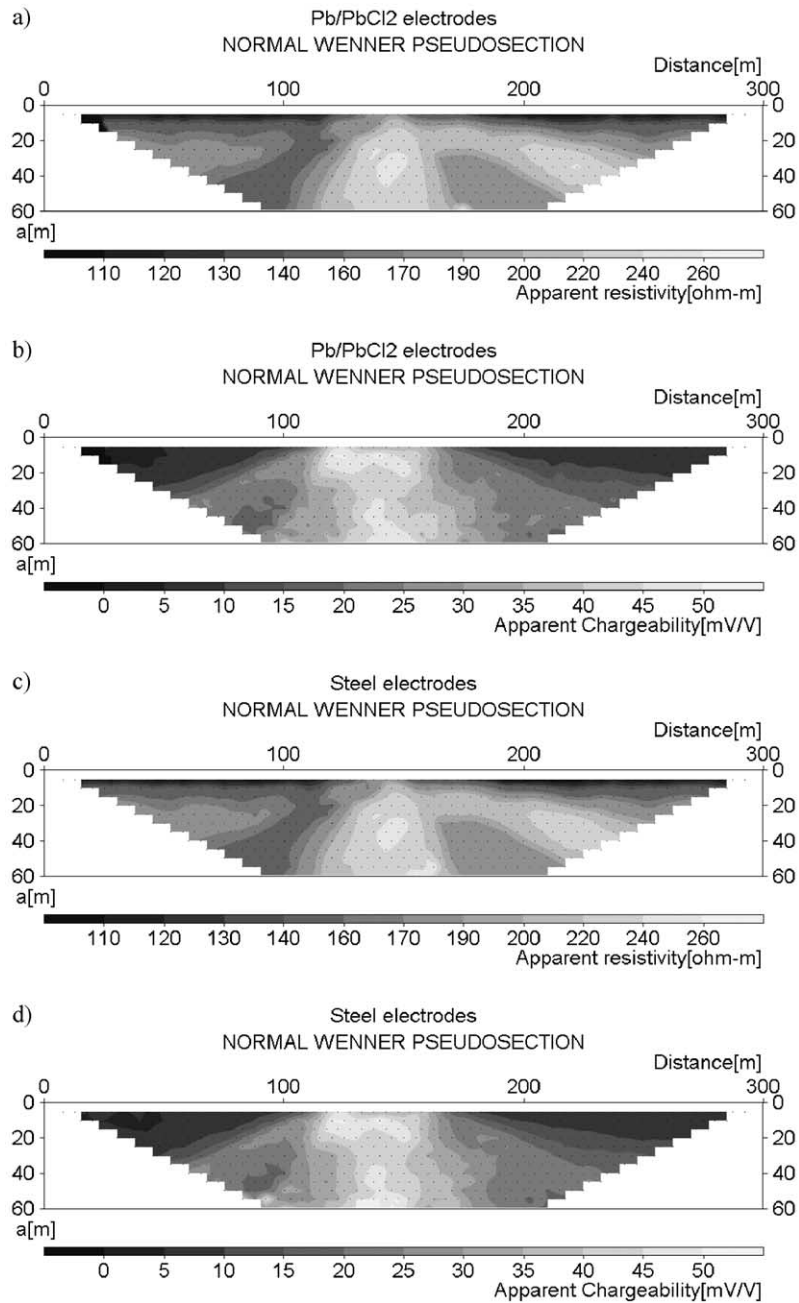
Fig. 17. Pseudosections measured with normal Wenner array at Östra Odarslöv. Time window approximately 20–120 ms after current turn-off used for the chargeability. (a) Apparent resistivity measured with lead chloride electrodes. (b) Apparent chargeability measured with lead chloride electrodes. (c) Apparent resistivity measured with steel electrodes. (d) Apparent chargeability measured with steel electrodes.

would have been much noisier if no correction had been done, as demonstrated in Fig. 14, which shows the same apparent chargeability pseudosection as the one in Fig. 9d, but without correction.

3.4. Inversion

The data was inverted to create a model of the resistivity and chargeability of the ground by using Res2dinv (ver. 3.50t). The inversion was done using least-squares optimisation (L2-norm). The resulting sections based on the steel electrode normal array data set are shown in Fig. 15. The inversion sharpens up the image from the pseudosections and focuses the low resistivities and high chargeabilities to the known location of the landfill. In this case, it is evident that the material in the landfill is characterised not only by low resistivity, but also by high chargeability. A few

zones of particularly high chargeability are visible at depth, which may be indicative of waste of a particular character. The exact reason for this is not clear; it may be due to a difference in the nature of the filling material or in its structure, or to different water content.

4. Östra Odarslöv test site

4.1. Site description

This test profile is located at Östra Odarslöv, a few kilometres north of Lund, Sweden. The site is characterised by a few metres of quaternary till resting on Silurian shale with dolerite intrusions (Fig. 16). Depth to the bedrock in the vicinity varies between 1.4 and 2.6 m according to drilling records. The
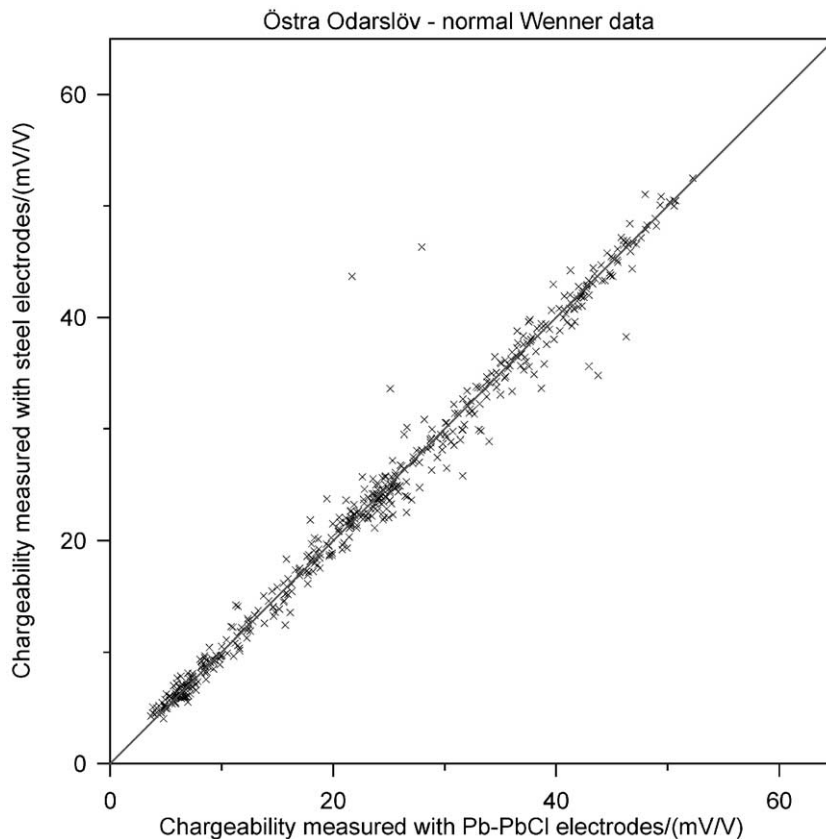

Fig. 18. Agreement between the normal Wenner chargeability values measured at Östra Odarslöv with stainless steel and lead chloride electrodes.
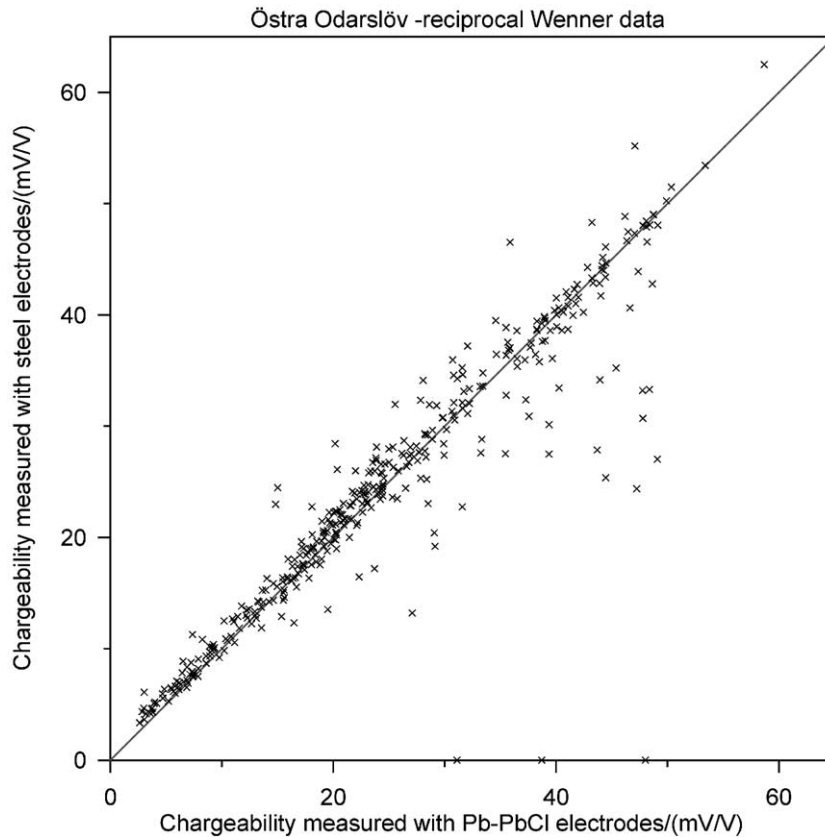
Fig. 19. Agreement between the reciprocal Wenner chargeability values measured at Östra Odarslöv with stainless steel and lead chloride electrodes.

topography is very gentle and reflects the bedrock topography, judged by drilling results and visual impressions in Östra Odarslöv quarry, situated immediately east of the test line. Drill-cores show grey shale throughout the drilled depths (15.56 and 25.12 m, respectively), with some calcite veins and pyritic zones. A dolerite dyke (approximately 20 m wide) was visible in the quarry before it was filled with building rubble some years ago. Furthermore, a slight change in the topographic slope along the profile can be seen where the dolerite dyke crosses (Dahlin, 1993). It may be noted that the line is passing below an AC power line.

4.2. Results

The measurements were carried out using Wenner electrode spacing ranging between 5 and 60 m. The

data sets with the different electrode types were recorded simultaneously using two channels in the instrument.

Table 3
Statistics on the errors in apparent chargeability from the Östra Odarslöv test line

Type of error	Steel electrodes		Pb/PbCl$_2$ electrodes	
	Absolute (mV/V)	Relative (%)	Absolute (mV/V)	Relative (%)
Number of data	388	388	389	389
Minimum	0.0	0.0	0.0	0.0
Maximum	26.7	100.6	18.9	96.8
Mean	2.9	12.5	2.3	12.0
Median	1.8	8.7	1.8	7.5
Standard deviation	3.7	13.2	2.1	13.2

Error estimates from difference between normal and reciprocal measurements for steel electrodes and lead chloride electrodes, respectively. Time window is 20–120 ms after current turn-off.

Table 4
Statistics on the errors in apparent chargeability from the Östra Odarslöv test line

Type of error	Normal Wenner		Reciprocal Wenner	
	Absolute (mV/V)	Relative (%)	Absolute (mV/V)	Relative (%)
Number of data	493	493	379	379
Minimum	0.0	0.0	0.0	0.0
Maximum	22.0	67.3	22.9	68.8
Mean	1.0	5.2	2.0	9.0
Median	0.7	3.1	1.1	5.3
Standard deviation	1.6	6.2	3.1	11.1

Error estimates from difference between measurements using steel and lead chloride potential electrodes for normal and reciprocal Wenner, respectively. Time window is 20–120 ms after current turn-off.

The results are presented as pseudosections of apparent resistivity and apparent chargeability in Fig. 17a–d, where the upper two sections show data recorded with lead–lead chloride electrodes and the lower ones corresponds for the steel electrodes. The time window for the calculation of the chargeabilities is 20–120 m after current turn-off. The dolerite dyke stands out as an anomalous feature with high resistivity and high chargeability. The apparent resistivity pseudosections (Fig. 17a and c) are very similar in appearance, with occasional noisy points in both. The apparent chargeability pseudosections (Fig. 17b and d) are also very similar in appearance, but with a slightly noisier appearance for the longest spacings in the steel electrode data set. For the apparent chargeabilities, a few outliers were removed before plotting the pseudosections (for both types of electrodes), whereas the apparent resistivities were plotted complete.

Figs. 18 and 19 give an explicit illustration of the agreement obtained between the chargeabilities measured with both kinds of electrodes for the normal and reciprocal arrays, respectively.

A closer comparison between the four corresponding apparent chargeability data sets is presented in Tables 3 and 4. The mean/median difference between normal and reciprocal measurements is 2.9/1.8 mV/V
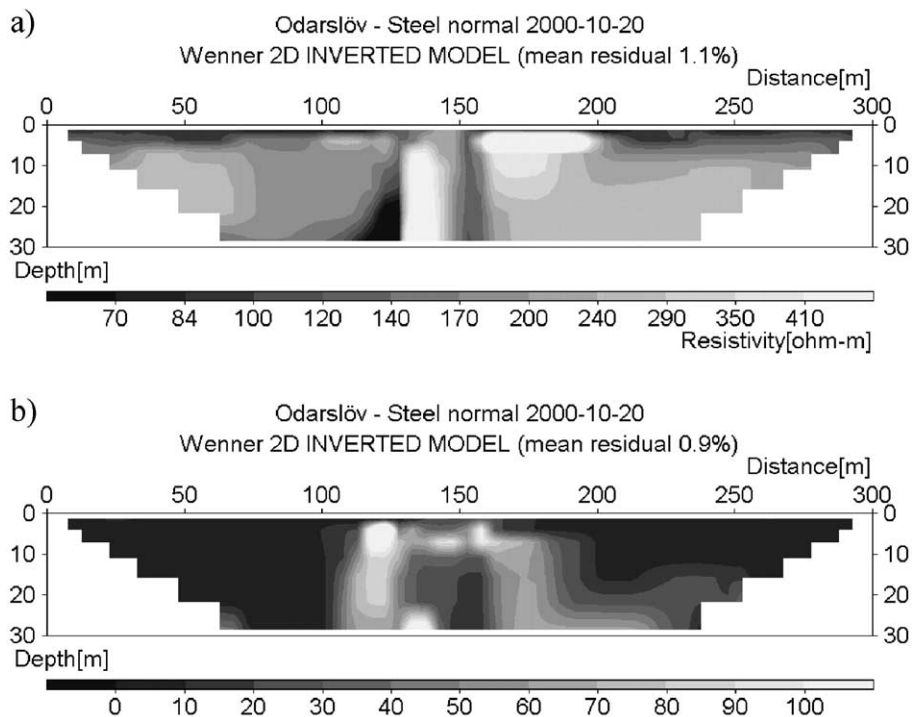

Fig. 20. Inverted sections based on data measured with normal Wenner array and steel electrodes at Östra Odarslöv. (a) Resistivity. (b) Chargeability.

for the steel electrodes, and 2.3/1.8 mV/V for the lead–lead chloride electrodes, respectively. This corresponds to a median relative discrepancy between normal and reciprocal measurements of 8.7% for the steel electrodes and of 7.5% for the lead–chloride ones. The comparison between the electrode types gives a difference of 1.0/0.7 mV/V for the normal array and 2.0/1.1 mV/V for the reciprocal array. The corresponding relative median discrepancies are 3.1% and 5.3%, respectively. Thus, the analysis shows that the agreement is better between the electrode types than the agreement between normal and reciprocal measurements for each type of electrode, which shows that the type of electrode used is not a critical factor at this site. It is also clear that the reciprocal data sets are noisier than the normal ones, which is again most likely explained by the longer potential electrode separations.

4.3. Inversion

The true subsurface distributions of resistivities and chargeabilities were estimated by inverting the pseudosections with Res2dinv (ver. 3.50t). In this case, the inversion was done using the robust inversion option in which the absolute differences are minimised (L1-norm). The resulting sections based on the steel electrode data are shown in Fig. 20. The dolerite dyke is enhanced as a feature of much higher resistivity than the surrounding rock, whereas the chargeability is increased in an area surrounding the dyke. This can be interpreted as IP-effects resulting from mineralisation in the contact metamorphism zone between the dyke and the surrounding rock.

5. Discussion and conclusions

In the two cases presented above, the addition of the chargeability allowed a better description of a natural target and of a man-made target. However, in order to allow a more widespread application of IP surveying in environmental and engineering applications, efficient field procedures are essential.

It has been demonstrated that, under the site conditions presented above, it is possible to use ordinary steel electrodes and the type of multicore cables used in DC resistivity imaging without degrading seriously the quality of the chargeability measurements.

Although nonpolarisable lead–lead chloride electrodes could generally be expected to give lower noise levels, the much more laborious and time-consuming field procedure is probably difficult to motivate in most cases of practical applications. Our results are encouraging for the possibility of less cumbersome and faster IP surveys.

The test sites used here are probably not particularly favourable from a noise point of view, since there are electrical power net cables crossing the line in both cases. The higher error level indicated for the reciprocal data sets may be a manifestation of this, the longer potential electrode separations picking up more noise. It is expected that there is a potential for further development concerning the resolution and noise suppression of the instruments, in terms of hardware as well as software.

Nevertheless, the electrode grounding conditions were favourable and the noise levels were not excessive at the test sites, thus the results may not necessarily be applicable to all environments. Based on the transmitted current levels and the specifications of the used transmitter, the maximum grounding resistances over the current electrode pairs are 4 $k\Omega$ or less at Dalby and 1 $k\Omega$ or less at Östra Odarslöv. It is difficult to define precisely what could be a favourable environment from such a limited number of case studies, but one could expect the grounding conditions and the conductivity of the soil to be the determining factors, since they control the level of the inductive coupling. Further research is needed with test measurements at various sites in order to draw more general conclusions.

The data from the Dalby site clearly demonstrate that electrode charge-up effects can be very significant, and that the quality of the results relies among other factors on the correction for these effects. It has been demonstrated that the effects can, to a large extent, be removed by the removal of a simple linear trend or of a second-order polynomial.

The detail of the coupling mechanisms deserves further studies, especially if we want to use multicore cables, since the level of the errors can be very serious in such a case. However, the moderate levels of measurement errors indicated by the analysis of the data presented above show that coupling effects have not been affecting data to any significant extent in this case.

One further step in the interpretation of the time-domain data could be to take advantage of the availability of the decay curve to extract the Cole–Cole parameters (following, for instance, Johnson, 1990), but in such a case, one needs to be aware of the possible effects on the frequency content of the low-pass filtering in the instrument, of the trend removal and of the kind of electrodes used. Similarly, the practical conclusions derived here may not be applicable when measuring IP in the frequency domain due to coupling problems.

Acknowledgements

References

Bernstone, C., Dahlin, T., 1997. Characterization of old landfills with the aid of DC-Resistivity. In: Proc. Sardinia '97, 6th International Landfill Symposium, 13–17 October, Cagliari, Italy, vol. IV, pp. 305–314.

Bertin, J., Loeb, J., 1976. Experimental and Theoretical Aspects of Induced Polarization. Volume I: Presentation and Application of the IP Method, Case Histories Gebrüder Borntraeger, Berlin.

Carlson, N.R., Mayerle, C.M., Zonge, K.L., 1999. Extremely fast IP used to delineate buried landfills. Procs. 5th Meeting of the European Association for Environmental and Engineering Geophysics, 5–9 September 1999, Budapest, 4 Chapter 3, 2 pp.

Dahlin, T., 1993. On the automation of 2D resistivity surveying for engineering and environmental applications. PhD thesis, Lund University, Sweden.

Dahlin, T., 1996. 2D resistivity surveying for environmental and engineering applications. First Break 14 (7), 275–283.

Dahlin, T., 2000. Electrode charge-up effects in DC resistivity data acquisition using multielectrode arrays. Geophysical Prospecting 48 (1), 181–187.

Effersø, F., Auken, E., Sørensen, K.I., 1999. Inversion of band-limited TEM responses. Geophysical Prospecting 47 (4), 551–564.

Griffiths, D.H., Turnbull, J., Olayinka, A.I., 1990. Two-dimensional resistivity mapping with a computer-controlled array. First Break 8 (4), 121–129.

Johnson, I.M., 1990. Spectral IP parameters derived from time-domain measurements. Induced Polarization Applications and Case Histories, Investigations in Geophysics, vol. 4. Soc. Explor. Geophys., Tulsa, OK, pp. 57–78.

Loke, M.H., 1999. Res2dinv ver. 3.4 for Windows 3.1, 95 and NT. Rapid 2-D resistivity and IP inversion using the least squares method, Software manual, http://www.abem.se.

Loke, M.H., Barker, R.D., 1996. Rapid least-squares inversion of apparent resistivity pseudosections by a quasi-Newton method. Geophysical Prospecting 44, 131–152.

Overmeeren, R.A. van, Ritsema, I.L., 1988. Continuous vertical electrical sounding. First Break 6 (10), 313–324.

Petiau, G., Dupis, A., 1980. Noise, temperature coefficient, and long time stability of electrodes for telluric observations. Geophysical Prospecting 28, 792–804.

Seigel, H.O., 1959. Mathematical formulation and type curves for induced polarization. Geophysics XXIV (3), 547–565.

Slater, L., Lesmes, D., 2002. IP interpretation in environmental investigations. Geophysics 67, 77–88.

Sumner, J.S., 1976. Principles of induced polarization for geophysical exploration. Developments in Economic Geology, vol. 5. Elsevier, Amsterdam (277 pp.).

Vacquier, V., Holmes, C.R., Kintzinger, P.R., Lavergne, M., 1957. Prospecting for groundwater by induced electrical polarisation. Geophysics 23, 660–687.

Vanhala, H., 1999. Comparison between geological models based on resistivity data and resistivity-IP data. Procs. 5th Meeting of the European Association for Environmental and Engineering Geophysics, 5–9 September 1999, Budapest, De8, 2 pp.

Vanhala, H., Soininen, H., 1995. Laboratory techniques for measurement of spectral induced polarization response of soil samples. Geophysical Prospecting 43, 655–676.

Wait, J.R., Gruska, T.P., 1986. On electromagnetic coupling "removal" from induced polarisation surveys. Geoexploration 24, 21–27.

Weller, A., Gruhne, M., Seichter, M., Börner, F.D., 1996. Monitoring hydraulic experiments by complex conductivity tomography. European Journal of Environmental and Engineering Geophysics 1, 209–228.